

Application of soft computing techniques in dental Image Segmentation

M.S.R. Naidu^{1*}, P. Rajesh Kumar²

Department of Electronics and communication Engineering

¹Aditya institute of technology and management (AITAM), Tekkali, Andhrapredesh, India

²A.U.College of engineering (A), Andhra university, Visakhaptnam, Andhrapredesh, India

Corresponding Author: M.S.R. Naidu

ABSTRACT

Image segmentation is a very important and pre-processing step in image analysis. The conventional multilevel thresholding methods are efficient for bi-level thresholding because of its simplicity, robustness, less convergence time and accuracy. However, a mass of computational cost is needed and efficiency is broken down as an exhaustive search is utilized for finding the optimal thresholds, which results in application of evolutionary algorithm and swarm intelligence to obtain the optimal thresholds. The main aim of image segmentation is to segregate the foreground from background. For the first time this paper established a naturally inspired hybrid optimization based multilevel image thresholding for image segmentation by maximizing Shannon entropy or Fuzzy entropy. The proposed algorithm is tested on standard set of medical dental images and it is demonstrated that the proposed method shows better performance in objective function, structural similarity index, and misclassification error than state of art methods.

Keywords: Image segmentation; Image thresholding; Fuzzy entropy; Shannon entropy; Cuckoo Search; Firefly algorithm; Gravitational search;

Date Of Submission:03-08-2018

Date Of Acceptance: 18-09-2018

I. INTRODUCTION

Segmentation is generally the first stage in any attempt to analyze or interpret an image automatically. Segmentation bridges the gap between low-level image processing and high-level image processing. Some kinds of segmentation technique will be found in any application involving the detection, recognition, and measurement of objects in images. The role of segmentation is crucial in most tasks requiring image analysis. The success or failure of the task is often a direct consequence of the success or failure of segmentation. However, a reliable and accurate segmentation of an image is, in general, very difficult to achieve by purely automatic means. Some of the applications of segmentation includes: Industrial inspection, Optical character recognition (OCR), Tracking of objects in a sequence of images Classification of terrains visible in satellite images, Detection and measurement of dental disease, tissue, etc., in medical images. In this paper, we propose new hybrid optimization technique for segmentation of dental images for better diagnosis of Ameloblastoma, Odontogenic Myxoma and Dentigerous Cyst diseases.

1. Ameloblastoma: -Ameloblastoma, is derived from the English word "amel" which means enamel and the Greek word "blastos" which means the germ. It arises from the epithelium of the dental lamina, and it is characterized by its local aggressive behavior and a high recurrence rate. Ameloblastoma was first described in 1827 by Cusack. In 1885, Malassez introduced the name "adamantinoma," which is presently used to illustrate a rare form of bone cancer described by Fisher in 1913. It was first detailed and described by Falkson in 1879. The term ameloblastoma was coined by Ivey and Churchill in 1930, a currently accepted term. It is considered as a true neoplasm as the name implies it mimics the cells of the enamel-forming organ. It was described by Robinson in 1937, as a benign tumor that is "usually unicentric, nonfunctional, intermittent in growth, anatomically benign and clinically persistent." The World Health Organization (WHO) (1991) defined ameloblastoma as a benign but locally aggressive tumor with a high tendency to recur, consisting of proliferating odontogenic epithelium lying in a fibrous stroma. In [1] authors reviewed about ameloblastoma of the jaw including publications from 1960 to 1993, and compared to the latest larger review. The occurrence of unicystic ameloblastoma has been studied in 20

patients presenting with unilocular cystic lesions whose clinical, radiographic and gross features were those of non-neoplastic cysts [2].

2. Odontogenic Myxoma: Odontogenic myxoma is a rare benign intraosseous neoplasm, which is called 'locally malignant' on account of its exceptionally high local aggressiveness, high recurrence rate and non-metastasizing nature.

Latest research reported that the average age for the odontogenic myxoma is 26.5 years, although majority of the investigators found that this lesion occurs in second or third decade of life. Most of the reports suggest that there is a slight female preponderance, mandibular predilection, and the lesion has a silent locally destructive nature. All these features were evident in our case. Our case, though a benign tumor, was a highly aggressive lesion, involving almost half of the mandible within a short span of one and a half years. Another interesting finding was that it did not cause much of a cortical expansion or facial deformity and appeared to be invading the bone antero-posteriorly, as well as displayed scalloping between the roots of the involved teeth, in much the same manner as an odontogenic keratocyst. Radiographically, the appearance of an odontogenic myxoma may vary from a unilocular radiolucency to a multilocular lesion, with a well-defined to diffuse margin. However, a unilocular appearance is more common among children and in anterior parts of the jaws. In tooth-bearing areas, the tumor is often scalloped between the roots and root resorption may occur, thus giving a false appearance of an OKC. However, the classical radiographic features of the odontogenic myxoma, where the bony trabeculae of a multilocular radiolucency intersect at right angles and the lesion causes root resorption, resulting in tooth mobility, were readily identifiable in our case. The typical soft, slippery and gelatinous nature of the specimen on macroscopic examination and the histopathological findings were also in accordance with the literature. Thus our case was a prototype of an odontogenic myxoma.

3. Dentigerous Cyst: Odontogenic cysts are a group of jaw cysts that are formed from tissues involved in odontogenesis (tooth development). Odontogenic cysts are closed sacs, and have a distinct membrane derived from rests of odontogenic epithelium. It may contain air, fluids, or semi-solid material. Intra-bony cysts are most common in the jaws, because the mandible and maxilla are the only bones with epithelial components. That odontogenic epithelium is critical in normal tooth development. However, epithelial rests may be the origin for the cyst lining later. Not all oral cysts are odontogenic cysts. For

example, mucous cyst of the oral mucosa and nasolabial duct cyst are not of odontogenic origin. In addition, there are several conditions with so-called (radiographic) 'pseudocystic appearance' in jaws; ranging from anatomic variants such as Stafne static bone cyst, to the aggressive aneurysmal bone cyst. Inflammatory cysts are considered as one of the most common odontogenic and non-odontogenic jaw lesions followed by dentigerous cyst. In a total of 7412 oral lesions, Khosravi et al. found that radicular inflammatory cysts are the most common jaw lesions accounting for 35.12% of the total odontogenic cysts reported in his study [3]. Although osteosarcoma is a rare neoplasm, its early detection is very important to improve the prognosis as the survival of patients with osteosarcoma is usually less than 5 years [4, 5]. Therefore, diagnosing jaw lesions and its early detection is one of the important challenges in oral health care [6, 7].

II. CONCEPT OF SHANNON AND FUZZY ENTROPY

Concept of Shannon Entropy: Entropy is the compressive procedure of information which results higher rate of compression and high speed of transmission which compresses the required number of bits depending on the observation of repetitive information/message. If there are $N = 2^n$ (if $N = 8$) messages to transmit, n ($n = 3$) bits are required, then for each of N messages, number of bits required is \log_2^N bits. If one observes the repetition of same message from a collection of N messages as well as the messages can be assigned a non-uniform probability distribution, it will be possible to use fewer than $\log N$ bits per message. This is introduced by Claude Shannon based on the Boltzmann's H-theorem and is called as Shannon entropy, Let X is random variable (discrete) with elements $\{X_1, X_2, \dots, X_n\}$, then probability mass function $P(X)$ is given as

$$H(X) = E[I(X)] = E[-\ln(P(X))] \quad (1)$$

Where E is the expected value operator, I show the content of information and $I(X)$ is also a random variable. Further the Shannon entropy is re-written as in Eq (2) and is considered as the objective function which is to be optimized with optimization techniques.

$$H(X) = \sum_{i=1}^n P(x_i) I(x_i) = - \sum_{i=1}^n P(x_i) \log_b P(x_i) \quad (2)$$

Where b base of the algorithm in general it is equal to 2. If $P(x_i) = 0$ for some i then the multiplier $0 \log_b 0$ is considered as zero, which is consistent with the limit.

$$\lim_{p \rightarrow 0^+} p \log(p) = 0 \quad (3)$$

The said equations are for discrete value of X and the same are applicable for continuous values of X by replacing summation with integer.

Concept of Fuzzy Entropy: Let $D = \{(i,j): i=0,1,2,\dots,M-1; j=0,1,2,\dots,N-1\}$ and $G = \{0,1,2,\dots,L-1\}$, Where M is width of image, N is height of image and L is number of gray level in image. $I(x,y)$ is the intensity of image at position (x,y) and $D_k = \{(x,y): I(x,y) = k, (x,y) \in D\}$, $k=0,1,2,\dots,L-1$. Let us assume two thresholds i.e. T_1, T_2 which divide the domain D of the original image into three regions such as E_d, E_m and E_b . E_d region covers the pixels whose intensity value is less than T_1 , E_m contains the pixels whose intensity is in between T_1, T_2 and E_b covers the pixels whose intensity is greater than T_2 . $\Pi_3 = \{E_d, E_m, E_b\}$ is an unknown probabilistic partition of D whose probability distribution. $P_d = P(E_d)$ $P_m = P(E_m)$ $P_b = P(E_b)$. μ_d, μ_m and μ_b are the membership functions (μ) of E_d, E_m and E_b respectively and require six parameters like $a_1, b_1, c_1, a_2, b_2, c_2$. The thresholds T_1 and T_2 values are variable based on the membership functions. The whole fuzzy entropy is calculated through summarizing fuzzy entropy of each class [8] i.e.

$$H(a_1, b_1, c_1, a_2, b_2, c_2) = H_d + H_m + H_b \quad (4)$$

As per the requirements of researchers, the two level thresholding can be extended to three or more and can be restricted to single level also. For two thresholds the number of parameters to be optimized is six and as levels of increasing number parameters to be optimized is also increasing, so fuzzy entropy takes much time for convergence. Hence two level image thresholding for image segmentation with the Shannon entropy and Fuzzy entropy proved to be efficient and effective but for multilevel thresholding, both entropy techniques consume much convergence time and increase exponential with level of thresholds. The drawback of Shannon entropy and Fuzzy entropy is convergence time. To improve the performance of these methods further and to reduce the convergence time, researchers used applications of optimization techniques such as differential evolution, Particle swarm optimization, Bat algorithm and hGSA-PS for image thresholding and henceforth image segmentation. These techniques are set to maximize the Shannon entropy and Fuzzy entropy as given in Eq (2) and (4).

III. OVERVIEW OF GRAVITATIONAL SEARCH ALGORITHM AND PATTERN SEARCH

3.1 Gravitational Search Algorithm (GSA): It is a metaheuristic optimization algorithm which is based on the Newton laws of gravity and motion [9]. In

GSA, performance of object is measured by its mass. The gravitational force causes a global movement of all objects towards the objects with heavier mass. The exploitation step of the algorithm is guaranteed because of the slow movement of the heavy masses than the lighter ones and these heavy masses correspond to good solution. Position, inertial mass, active gravitational mass, and passive gravitational mass are the four specifications of each mass in GSA and each mass offers a solution. By lapse of time the heavier mass may attract the masses and this represents the optimum solution in the search space [8].

3.2. Pattern Search Algorithm: Pattern search is a heuristically search method that can be applied when the given objective function is neither continuous nor differentiable or when we are not aware of the information [10]. It only depends on the functional value at a point of concern. However, it can be applicable to both the differentiable as well as non-differentiable function; in general it is applied for the latter case, since in the differentiable case, it would rather leave all the useful information about the first derivative and the second derivatives. Thus, pattern search is also called derivative-free, direct search (or) black box optimization methods [8].

IV. RESULTS AND DISCUSSION

For the performance evolution which includes robustness, efficiency and convergence of proposed hybrid gravitational search and pattern search algorithms, we selected "Dentigerous Cyst, Odontogenic Myxoma and Ameloblastoma" as a test images. These images are obtained from the clinic which is located in Visakhapatnam, Andhrapradesh and all are .jpg format images and of size 256×255 and corresponding histograms are shown in Fig. 1. In general, perfect threshold can be selected if the histogram of image peaks is tall, narrow, symmetric, and separated by deep valleys. Odontogenic Myxoma and Ameloblastoma image histograms peaks are tall, narrow and symmetric, but for Dentigerous Cyst image histogram peaks are not tall and narrow so difficult to segment with ordinary methods. So we proposed hGSA-PS based image thresholding for effective and efficient image segmentation of above said critical images by optimizing Shannon and Fuzzy entropy. The performance and effectiveness of proposed gravitational search algorithm proved better compared to other optimization techniques like FA and ACS.

4.1. Maximization of Shannon and Fuzzy entropy

The HGSA-PS and other two algorithms are applied on Shannon and Fuzzy entropy objective function and compared the results of FA and ACS. All the algorithms are optimized to maximize the objective function. Table. 1 show the objective values of HGSA-PS, ACS and FA. It is observed from Table. 1 that objective values obtained with HGSA-PS by using Shannon and Fuzzy entropy is higher than the FA and ACS for different images.

4.2. Misclassification error/Uniformity measure:

It is measure of uniformity in threshold image and is used to compare optimization techniques performance. Misclassification error is measured by Eq. 5

$$M = 1 - 2 * Th * \frac{\sum_{j=0}^{Th} \sum_{i \in R_j} (I_i - \sigma_j)^2}{N * (I_{max} - I_{min})^2} \tag{5}$$

Where Th is the number of thresholds which are used to segment the image, R_j is the jth segmented region, I_i is the intensity level of pixel in that particular segmented area, σ_j is the mean of jth segmented region of image, N is total number of pixels in the image, I_{min} and I_{max} are the maximum and minimum intensity of image respectively. In general misclassification errors lies between 0 and 1 and higher value of misclassification error shows better performance of the algorithm. Hence, the Uniformity measure in thresholding is measured from the difference between the maximum value, 1 (better quality of image) and minimum value, 0 (worst quality of image). Table. 2 shows misclassification error of proposed and other techniques and proved proposed method have lesser misclassification error and shows better visual quality.

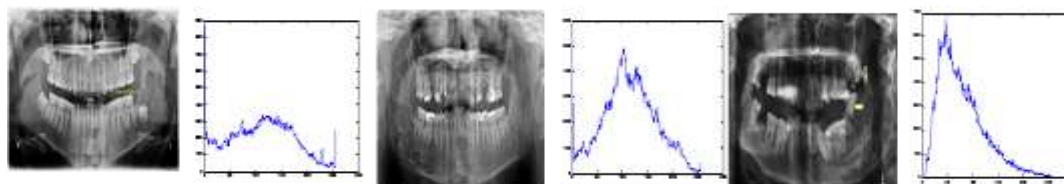


Fig.1. Standard image and respective histograms of three methods a) Dentigerous Cyst b)Ameloblastoma

c) OdontogenicMyxoma

Table 1

Comparison of objective values obtained by various algorithms

Ima	Opt	Th = 2		Th = 3		Th = 4		Th = 5	
		Shannon	Fuzzy	Shannon	Fuzzy	Shannon	Fuzzy	Shannon	Fuzzy
1	FA	10.5714	13.1337	10.5714	16.44282	14.5383	22.3239	14.5543	22.3239
	ACS	10.6235	14.0753	10.8433	16.99897	15.18976	22.8674	14.5616	22.5098
	hGSA-PS	10.7665	14.5876	11.1345	17.0897	15.3453	22.9754	14.7865	22.9876
2	FA	10.4291	12.9307	10.4291	16.2072	14.4685	19.2195	14.4681	23.1822
	ACS	10.5949	13.0202	10.5362	16.3992	14.6282	19.2829	14.53838	23.4944
	hGSA-PS	10.6373	13.3332	10.6717	16.3737	14.7838	19.3838	14.6272	23.5363
3	FA	9.92901	12.8331	10.2373	16.1222	12.2211	19.1639	13.2928	21.9452
	ACS	10.0897	12.7654	10.0987	16.0987	12.1274	19.2878	13.0909	22.1089
	hGSA-PS	10.4343	12.6784	10.3421	16.2908	12.3568	19.3565	13.1897	22.3456

Table 2

Comparison of Misclassification error values obtained by various algorithms

Ima	Opt	Th = 2		Th = 3		Th = 4		Th = 5	
		Shannon	Fuzzy	Shannon	Fuzzy	Shannon	Fuzzy	Shannon	Fuzzy
1	FA	0.77082	0.95904	0.65623	0.93884	0.78962	0.86437	0.73216	0.77411
	ACS	0.76543	0.94002	0.64321	0.82761	0.77342	0.85324	0.72637	0.75643
	hGSA-PS	0.75744	0.92341	0.63453	0.80901	0.75675	0.84321	0.70865	0.74567
2	FA	0.83883	0.96390	0.75824	0.94698	0.84033	0.86778	0.80041	0.70031
	ACS	0.82345	0.95432	0.76432	0.93456	0.83572	0.85432	0.79987	0.69087
	hGSA-PS	0.81356	0.94665	0.75676	0.92874	0.82791	0.84796	0.78421	0.65884
3	FA	0.76542	0.96365	0.66764	0.96810	0.70879	0.95329	0.89786	0.91864
	ACS	0.75897	0.97651	0.65788	0.95678	0.69087	0.94567	0.87896	0.90156
	hGSA-PS	0.74567	0.96789	0.64565	0.94567	0.68764	0.93456	0.86543	0.89078

4.3. Structural Similarity Index (SSIM)

It estimates the visual likeness between the input image and the decompressed image/thresholded image and is calculated with below equation

$$SSIM = \frac{(2\mu_I\mu_{\tilde{I}} + C1)(2\sigma_{I\tilde{I}} + C2)}{(\mu_I^2 + \mu_{\tilde{I}}^2 + C1)(\sigma_I^2 + \sigma_{\tilde{I}}^2 + C2)} \quad (6)$$

Where μ_I and $\mu_{\tilde{I}}$ are the mean value of the input image I and decompressed image \tilde{I} , σ_I and $\sigma_{\tilde{I}}$ are the standard deviation of original image I and reconstructed image \tilde{I} , $\sigma_{I\tilde{I}}$ is the cross-correlation and $C1$ & $C2$ are constants which are equal to 0.065. Table. 3 shows the SSIM of various methods with Shannon and Fuzzy entropy and it demonstrate proposed method SSIM is higher than other methods. Fig. 2 shows the segmented images and respective optimized 5 level thresholds with HGSA-PS and it shows segmentation with HGSA-PS is better than FA and ACS.

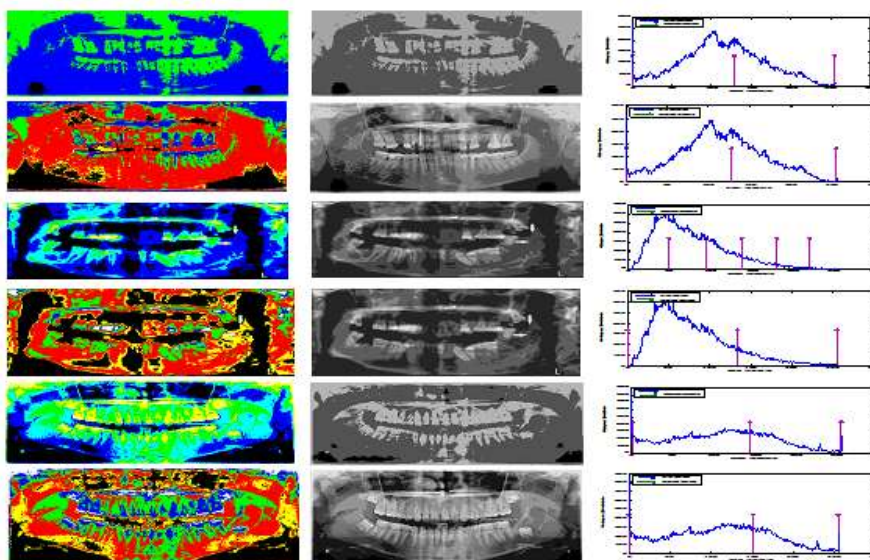


Fig.2. Segmented images and respective optimized 5 level thresholds with hGSA-PS

Table 3
 Comparison of SSIM obtained by various algorithms

Ima	Opt	Th = 2		Th = 3		Th = 4		Th = 5	
		Shannon	Fuzzy	Shannon	Fuzzy	Shannon	Fuzzy	Shannon	Fuzzy
1	FA	0.22147	0.54386	0.22147	0.72610	0.46671	0.72610	0.46581	0.77647
	ACS	0.23478	0.55908	0.23789	0.73678	0.45013	0.73468	0.46666	0.78564
	hGSA-PS	0.24988	0.56897	0.24897	0.74879	0.46780	0.74789	0.47890	0.79021
2	FA	0.30477	0.53644	0.30477	0.63808	0.48186	0.75908	0.48181	0.80675
	ACS	0.31089	0.54786	0.31567	0.65678	0.49076	0.77654	0.49089	0.81378
	hGSA-PS	0.32467	0.56897	0.32486	0.67543	0.51890	0.79843	0.51687	0.87654
3	FA	0.33676	0.56826	0.34393	0.67816	0.539292	0.71946	0.52399	0.74485
	ACS	0.34838	0.54383	0.31393	0.65959	0.528823	0.70948	0.51981	0.73939
	hGSA-PS	0.36392	0.57555	0.34849	0.68444	0.54595	0.72727	0.53838	0.74363

V. CONCLUSIONS

In this paper, we proposed natural inspired adaptive cuckoo search algorithm based multilevel image thresholding for image segmentation. hGSA-PS maximizes the Fuzzy and Shannon entropy for efficient and effective image thresholding. The proposed algorithm is tested on dental images to show the merits of the algorithm. The results of the proposed method are compared with other optimization techniques such as FA and ACS with

Shannon and Fuzzy entropy. From the experiments we observed that proposed algorithm has higher/maximum fitness value compared to FA and ACS. The SSIM value shows higher values with proposed algorithm than FA and ACS. It is concluded that proposed algorithm outperform the FA and ACS in all performance measuring parameters.

REFERENCES:

- [1]. P.A.Reichert, H.P.Philipsen, S.Sonner, "Ameloblastoma: Biological profile of 3677 cases", *European Journal of Cancer Part B: Oral Oncology*, Vol., No. 2, 86-99, 1995.
- [2]. Leonard Robinson, Mario G. Martinez, "Unicystigameloblastoma. A prognostically distinct entity", *Head & Neck*, Vol. 39, No. 5, pp. 996-1000, (2017).
- [3]. Khosravi N, Razavi SM, Kowkabi M, Navabi AA. Demographic distribution of odontogenic cysts in Isfahan (Iran) over a 23-year period (1988–2010). *Dent Res J* 2013;10(2):162–7.
- [4]. Rajendran R. Shafer's textbook of oral pathology. 6th ed, 2009.
- [5]. Bhadage C, Vaishampayan S, Kolhe S, Umarji H. Osteosarcoma of the mandible mimicking an odontogenic abscess: a case report and review of the literature. *Dent Update* 2013;40(3):216–21.
- [6]. Santhosh B. Review on emerging techniques to detect oral cancer. *Int J ElectrSciEng* 2015;1(1):41–6.
- [7]. Sharma N, Om H. Significant patterns for oral cancer detection: association rule on clinical examination and history data. *Netw Model Anal Health Inform Bioinform* 2014;3(1):1–13.
- [8]. M.S.R. Naidu, P. Rajesh Kumar, "Hybrid Gravitational Search Algorithm and Pattern Search based Evolutionary Image Thresholding for Image Segmentation", *International Journal of Digital Content Technology and its Applications (JDCTA)*, Vol. 11, No. 1, 2017.
- [9]. Rashedi. E, Nezamabadi-pour. H, Saryazdi. S, "Filter modeling using gravitational search algorithm", *Engineering Application of Artificial Intelligence*, Vol. 24, pp. 117–122, 2011.
- [10]. Dolan, E.D., Lewis, R.M. and Torczon, V, "On the local convergence of pattern search", *SIAM Journal of Optimization*, Vol. 14, No. 2, pp. 567–83, 2003.

M.S.R. Naidu "Application of soft computing techniques in dental Image Segmentation " *International Journal of Engineering Research and Applications (IJERA)* , vol. 8, no.9, 2018, pp 45-50